Reconfigurable Trans-Inductor Voltage Regulator with Improved Light Load Efficiency in Data Center Applications

Ziyao Wang, Zehui Li and Haoyu Wang
School of Information Science and Technology
ShanghaiTech University, Shanghai, China
Shanghai Engineering Research Center of Energy Efficient and Custom AI IC
wanghy@shanghaitech.edu.cn

2025 IEEE Applied Power Electronics Conference and Exposition (APEC) | 979-8-3315-1611-6/25/$31.00 ©2025 IEEE | DOI: 10.1109/APEC48143.2025.10977329

***Abstract*—In data centers, the trans-inductor voltage regulator (TLVR) is emerging as a promising topology for point-of-load converters, designed to deliver high-current, fast-transient power to the XPU. Since XPUs typically operate under light load conditions, enhancing TLVR light load efficiency is essential. This paper proposes a novel reconfigurable TLVR design that incorporates a 4-quadrant switch within the secondary side coupling loop of the trans-inductor. At heavy load, the configuration retains the characteristics of a conventional TLVR. While at light load, the TLVR is reconfigured to decouple the interleaved phases, thus improving light load efficiency. A 12V/1.8V, 500kHz, 80A 4-phase TLVR with this secondary switch was designed and tested, with experimental results demonstrating an average light load efficiency improvement of 2.9%.**

***Index Terms*—data center, light load efficiency, TLVR, voltage regulator modules.**

I. Introduction

With the rapid development of cloud computing, big data, and artificial intelligence, the energy consumption of data centers is booming. It uses about 2% of the global electricity supply and will grow to 4% $\sim$ 8% by 2030 [1]. However, the load point XPUs operate in idle mode for over 89% of the time, with power consumption at less than 10% of full load capacity [2]. Therefore, enhancing light load efficiency is crucial for energy saving in data centers.

In point-of-load applications, there is a high demand for the ability to handle large currents and fast current slew rates. The trans-inductor regulator (TLVR) topology is a ideal candidate, offering reduced conduction losses, output current ripple cancellation, and improved dynamic response [3] [4]. However, as a coupled inductor buck-derived converter, TLVR suffers from low light-load efficiency due to the inter-phase coupling and the high step-down conversion ratio. This coupling introduces additional driving and conduction losses [5]. Moreover, high step-down buck converters face challenges such as low duty cycle and hard switching, which further degrade the efficiency [6]. Narrow duty cycles increase output voltage sensitivity, complicate control and gate drive design, and lead to higher RMS current, exacerbating conduction losses [7]. Switching losses are increased, and the benefits of interleaving are diminished [8].

Several techniques have been proposed to enhance efficiency, particularly to extend their duty cycles. Cascading converters offer a straightforward method to achieve a higher duty cycle but increase the component count and control complexity, which ultimately reduces efficiency [9]. In [10], quadratic topologies combining series converters are proposed to reduce switch count. However, they still suffer from high voltage and current stress on the switches, which impacts overall performance. In [11] [12], another series capacitor-based technique is proposed to extend the duty cycle, reduce voltage stress on MOSFETs, and ensure current balance across phases. However, this approach faces challenges such as hard switching of MOSFETs and increased circuit complexity due to a larger number of components. To mitigate switching losses, series-resonant structures are investigated in series capacitor converters [13]. However, hard switching in high-side MOSFETs and zero current switching (ZCS) in low-side MOSFETs remain challenges, with zero voltage switching (ZVS) required to eliminate the switching losses.

Other methods address issues associated with coupled inductors. In [5], synchronized control of two coupled inductor phases is proposed. It eliminates power loss from dual zero current touching, but the current ripple increases. In [14], a tapped-inductor-based converter is studied to extend the duty cycle and reduce switching stress. However, leakage inductance in the tapped inductor often resonates with switches' parasitic capacitance which limits the overall performance. In [15], lossless snubber and active clamp circuit are used to reduce ringing and achieve soft switching, but this adds complexity. Another drawback of coupled inductor converters is the pulsating output current in [14] [15], which leads to excessive equivalent series resistance (ESR) losses in the output capacitance and reduces its lifespan [16]. In [17], a new coupled inductor structure with shorter winding paths is proposed to suppress the magnetic loss. Still, the asymmetry in the multi-phase structure results in unequal phase-coupling coefficients, leading to unbalanced phase ripple current cancellation and larger output capacitors. Additionally, nonlinear inductors have been suggested to enhance light load efficiency in [18] [19]. By increasing inductance, current ripple-related

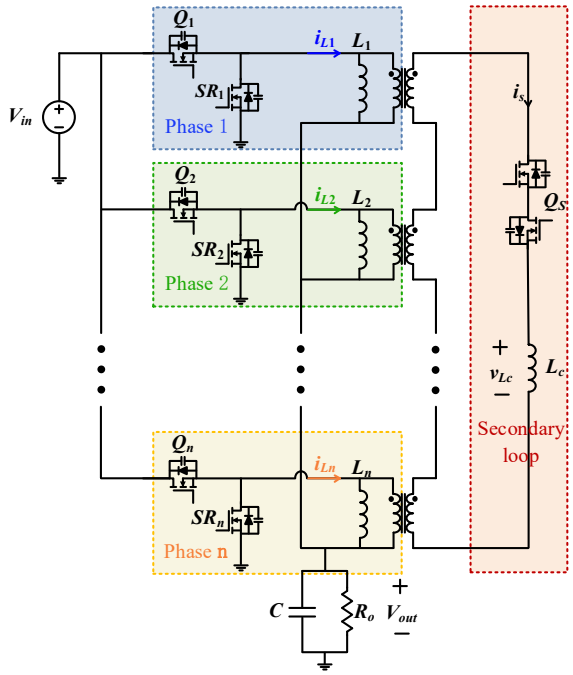

Fig. 1. Schematic of the proposed reconfigurable TLVR.

losses at light load can be minimized, although the magnetic design becomes more complex.

In this paper, we propose a novel reconfigurable TLVR designed to enhance light load efficiency. By incorporating a four-quadrant switch into the coupling loop on the secondary side of the trans-inductor, our design facilitates dynamic phase coupling control. During heavy loads, the switch is turned on to support conventional TLVR operation, ensuring a rapid transient response. Under light load conditions, the switch deactivates, decoupling the TLVR phases. This strategy not only optimizes phase shedding, but also increases the equivalent steady-state inductance, thereby reducing current ripple and associated losses, leading to improved light load efficiency. Compared to existing approaches, our solution boasts a simplified structure, ease of implementation, straightforward control, and excellent scalability, making it suitable for high-power applications.

The remainder of this paper is structured as follows. Section II outlines the reconfigurable TLVR and explains its operation principles. Section III delves into the methodology for improving light load efficiency. Section IV presents a loss analysis model to demonstrate the effects of our proposed solution on overall system losses. Experimental results are provided in Section V. Lastly, Section VI concludes the paper.

II. Proposed Reconfigurable TLVR

The schematic of the proposed reconfigurable TLVR is shown in Fig. 1. The primary side consists of an interleaved multi-phase buck converter, where each phase includes a half-bridge and a transformer. The primary winding is connected between the half-bridge switching point and the output, while all secondary windings are connected in series with a compensating inductor L_c, and an additional switch Q_s. This design builds on the conventional TLVR framework by adding a reconfigurable component: a four-quadrant switch Q_s, positioned in the coupling loop on the secondary side of the trans-inductor. In practice, Q_s is implemented using two back-to-back MOSFETs to control phase coupling. The operational principle of the reconfigurable TLVR is illustrated in Fig. 2. Depending on the load condition, the converter offers two operation modes as follows.

A. Heavy-load Mode

At heavy loads, the circuit operates in continuous conduction mode (CCM). The secondary switch is turned on to maintain phase coupling, preserving the characteristics of a conventional TLVR. For a 4-phase example, when any phase on the primary side is activated, the voltage across the secondary inductor L_c is $V_{in} - 4V_{out}$; when all phases are deactivated, it becomes $-4V_{out}$. This voltage determines the secondary current i_{Lc}. The TLVR inductor current i_L can be viewed as the superposition of i_{Lc} and the inductor current of uncoupled buck, as illustrated in Fig. 3.

B. Light-load Mode

At light load, the secondary switch is turned off, disconnecting the secondary coupling circuit. Without the influence of secondary current, the converter is reconfigured to function as a multi-phase buck converter, inheriting its characteristics. This mode effectively reduces power loss. A detailed analysis is provided in Section III.

C. Effect of Switch

The equivalent circuit in the secondary loop is shown in Fig. 4, assuming that the leakage inductance of the coupled inductor is negligible.

In heavy-load mode, Q_s is turned on and can be treated as a resistor R_{eq}, representing the on-resistance of the two MOSFETs. This additional resistance contributes to conduction losses. To evaluate its effect on overall efficiency, we first calculate the secondary current. Using the previously mentioned voltage, the effective value of the secondary current is derived as follows:

$$I_{s-heavy} = \frac{(1-4D)V_{out}}{2\sqrt{3}L_c f_s} \tag{1}$$

As shown in (1), $I_{s-heavy}$ is independent of the load. When the output current increases, the additional losses introduced by the secondary switch remain constant, represented by $I^2_{s-heavy}R_{eq}$. However, since the calculated value of $I_{s-heavy}$ is much smaller than the heavy-load current, this extra conduction loss accounts for less than 1% of the primary-side MOSFET losses, making it negligible in terms of overall performance.

In light-load mode, we aim to reduce the secondary current to zero to fully decouple the phases. However, when Q_s is

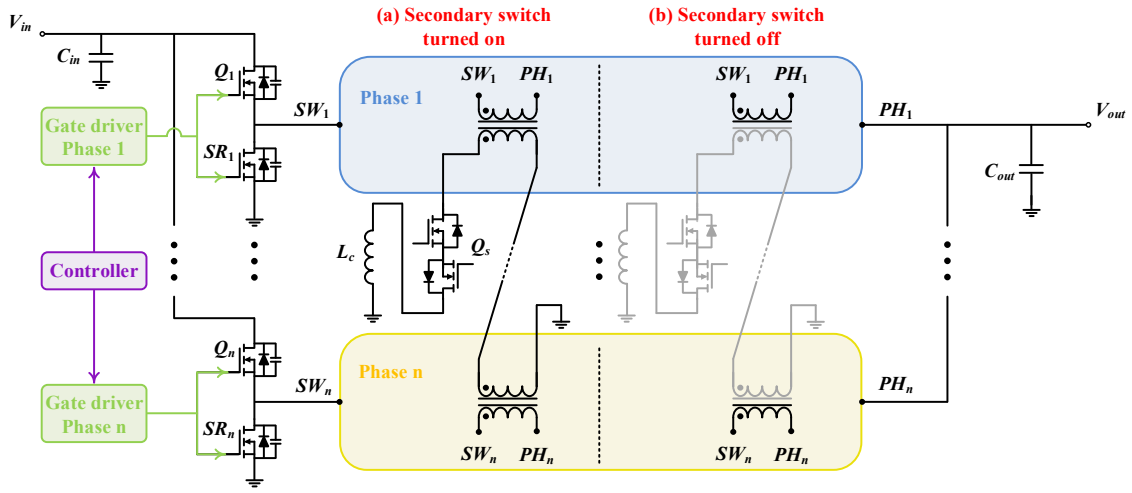

Fig. 2. Operation principle of reconfigurable TLVR.

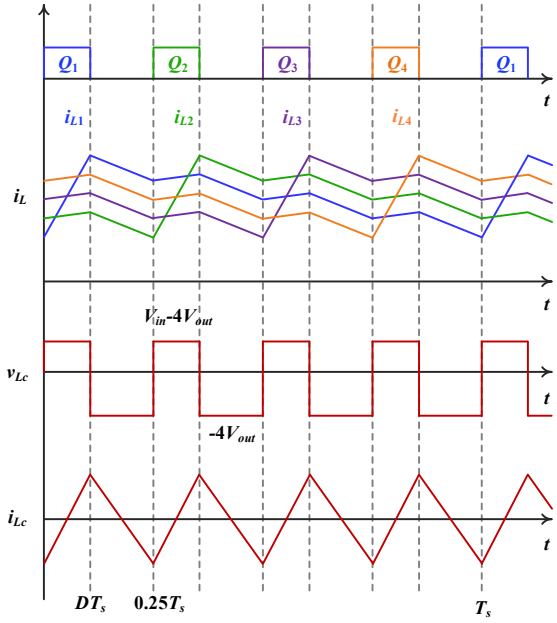

Fig. 3. Main converter waveforms for the proposed reconfigurable TLVR in heavy-load mode.

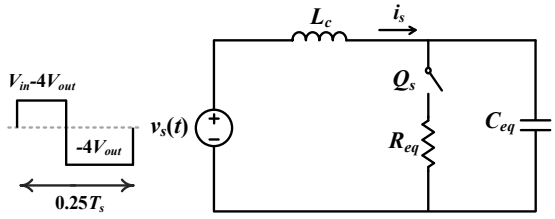

Fig. 4. Equivalent circuit in the secondary loop.

turned off, the output capacitors of the MOSFETs (represented as C_{eq} in Fig. 4) remain in the secondary loop, potentially causing a resonant current. The impedance in circuit can be represented as $j\omega L_c + 1/j\omega C_{eq}$. The effective value of the resonant current can be calculated as

$$I_{s-light} = \frac{V_{Lc}}{|\omega L_c - \frac{1}{\omega C_{eq}}|} \tag{2}$$

To ensure this resonant current does not affect the primary current, we can select MOSFETs such that the output capacitance satisfies $I_{s-light} < 0.01A$, which is much smaller than the primary current. In this case, we can treat the resonant current as negligible, considering the secondary loop as an open circuit.

III. Light Load Efficiency Improvement Method

A. Enhanced Phase Shedding

In multi-phase Buck converters, phase shedding is commonly used to improve light load efficiency by reducing switching loss, core loss, and driving loss through a reduction in the number of active phases [20] [21]. However, in conventional TLVR, the efficiency gains from phase shedding are limited due to phase coupling. When one phase is ON (with its upper MOSFET turned on) and the redundant phases are OFF (with their upper MOSFETs turned off), a coupled current still flows in the OFF phases by the conduction of secondary loop, as shown in Fig. 5. This current introduces additional losses. If the synchronous rectifier (SR) channel is off, the coupled current flows through the SR body diode, causing

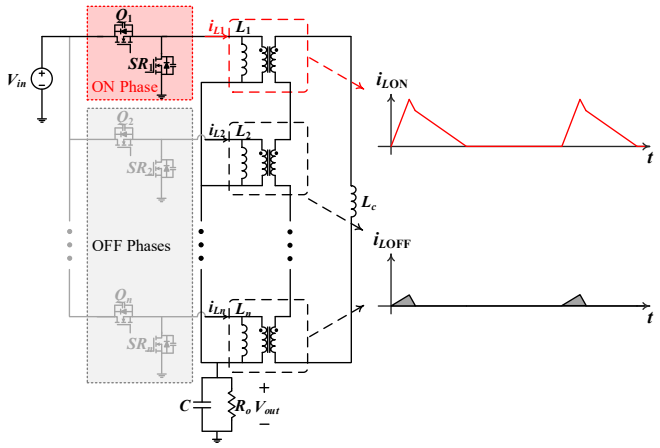

Fig. 5. Inductor current waveforms of TLVR with phase shedding.

extra conduction losses. If the SR channel is on, driving losses increase. The proposed reconfigurable TLVR addresses this issue by turning off the secondary switch, which decouples the phases and eliminates the coupling current in the OFF phases, thereby improving light load efficiency.

B. Increased Equivalent Steady-state Inductance

Decoupling the phases increases the equivalent steady-state inductance of the circuit, which helps reduce ripple-related losses and improve efficiency. The steady-state equivalent inductance of an *n*-phase coupled inductor is introduced in [22] and shown in (3).

$$L_{ss} = \frac{(L_{self} - M)(L_{self} + (n-1)M)}{L_{self} + (\frac{n-1}{1-D} - 1)M} \tag{3}$$

where L_{self} is the self-inductance, and M is the mutual inductance coefficient, which can be calculated as:

$$L_{self} = (1 - \frac{k^2}{n+\beta})L_{nc} \tag{4}$$

$$M = -\frac{k^2}{n+\beta}L_{nc} \tag{5}$$

Here L_{nc} represents the inductance of each phase when the coupled winding loop is open, $L_{nc} = L_m + L_k$, with L_m is the magnetic inductance,L_k is the leakage inductance. k is the coupling coefficient, $k = L_m/L_{nc}$, and $\beta = L_c/L_{nc}$. According to (3)–(5), it is evident that the mutual inductance coefficient M directly influences the steady-state inductance L_{ss}. When phases are coupled, $(M \neq 0)$, L_{self} can be calculated using (4). When phases are decoupled $(M = 0)$, L_{self} equals L_{nc}, which is larger than the L_{self} calculated from (4). This results in an increased L_{ss}, and a larger L_{ss} leads to reduced current ripple, thereby lowering conduction losses.

IV. Power Loss Analysis at Light Load

A. Core Loss

In this paper, we decouple the secondary loop and simultaneously enable phase shedding at light load. As a result, the secondary-side current approaches zero, and only the magnetic loss of the ON phase and the primary copper loss need to be considered. The magnetic flux variation can be derived as

$$\Delta B = \frac{L\Delta i}{2nA_e} \tag{6}$$

where n is the winding turns and A_e is the effective cross-sectional area of the magnetic core. The transformer core loss can be expressed as

$$P_{core} = V_c k f_s^x \Delta B^y \tag{7}$$

where V_c is the core volume, k, x, y are coefficients determined by the core material, which can be derived in dataset. The total inductor loss can is the sum of core loss and winding loss, expressed as

$$P_{inductor} = P_{core} + I_{rms}^2 R_{winding} \tag{8}$$

where I_{rms} is the effective value of load current, and $R_{winding}$ is resistance of the primary winding.

B. ON-phase MOSFET Losses

The ON-phase MOSFET losses constitute the primary portion of light load losses. These include switching losses (P_{sw}), driving losses (P_{dri}), and the conduction losses (P_{cond}) in the upper and lower MOSFETs. The switching losses are given by:

$$P_{sw} = \frac{1}{2}V_{ds}I_{ds}(t_{on} + t_{off})f_s \tag{9}$$

where t_{on} and t_{off} are the turn-on and turn-off times of the MOSFETs, which can be approximated by the following equations [2]:

$$t_{on} = R_G C_{iss} \ln\frac{V_{gs} - V_{th}}{V_{gs} - V_{gp}} + R_G C_{gd}\frac{V_{ds}}{V_{gs} - V_{gp}} \tag{10}$$

$$t_{off} = R_G C_{iss} \ln\frac{V_{gp}}{V_{th}} + R_G C_{gd}\frac{\Delta Q_{ds}}{\Delta V_{ds}}\frac{V_{ds}}{V_{gp}} \tag{11}$$

The driving losses are expressed as:

$$P_{dri} = Q_g V_{gs} f_s \tag{12}$$

Finally, the conduction losses can be calculated as:

$$P_{cond} = \int_0^{T_s} I_{ds-on}^2 dt \times R_{ds-on} f_s \tag{13}$$

where R_G is the gate resistance, C_{iss} is the input capacitance, V_{gs} is the gate-source voltage, V_{gp} is the gate plateau voltage, V_{th} is the gate threshold voltage, C_{gd} is the gate-drain capacitance, and Q_g is the gate charge. ΔQ_{ds} and ΔV_{ds} represent the changes in the drain-source charge and voltage, respectively.

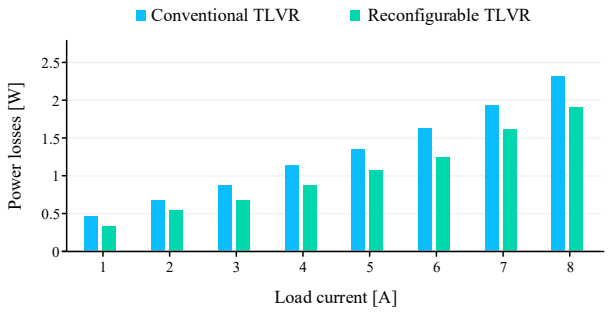

Fig. 6. Comparison of light load losses between the conventional TLVR and the reconfigurable TLVR.

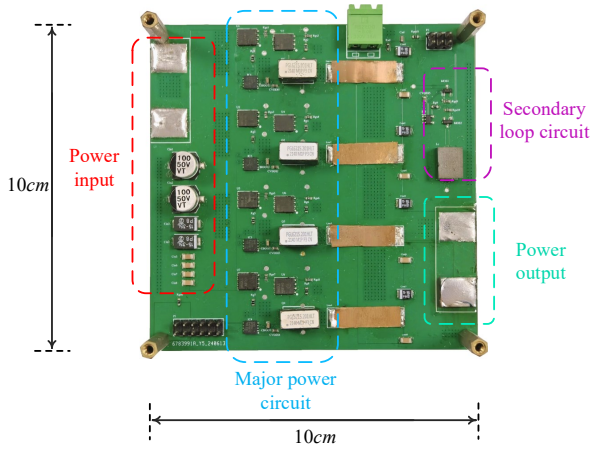

Fig. 7. Prototype of the reconfigurable TLVR.

C. OFF-phase MOSFET Losses

For the OFF phases, losses occur when no driving signal is provided, allowing the MOSFET's body diode to conduct the coupled current. The losses in this case include the conduction loss $P_{cond-BD}$ and the recovery loss P_{rr} of the body diode. The conduction loss in the body diode is given by:

$$P_{cond-BD} = V_F \cdot I_D + I_D^2 \cdot R_F \tag{14}$$

where V_F is the forward voltage drop of the body diode, I_D is the current through the body diode, and R_F is the resistance to the body diode. The recovery loss, due to the reverse recovery charge of the body diode, is:

$$P_{rr} = Q_{rr} V_{ds} f_s \tag{15}$$

where Q_{rr} is the reverse recovery charge of the body diode, and V_{ds} is the drain-source voltage.

In summary, the total losses as a function of load current for both the reconfigurable TLVR and the conventional TLVR are compared in Fig. 6. The reconfigurable TLVR reduces losses and improves light load efficiency when the secondary switch is turned off.

TABLE I
COMPONENTS AND CIRCUIT PARAMETERS

Parameter	Value
Input Voltage	12V
Output Voltage	1.8V
Load Current(full load)	80A
Phase Number	4
Switching Frequency	500kHz
Controller	TMS320F28335
Coupled Inductor	PGL6215.201HLT
Primary-side MOSFET	BSC0802LS
Primary-side Driver	2EDL8024G
Secondary-side MOSFET	DMN2053
Secondary-side Driver	1EDN7512B

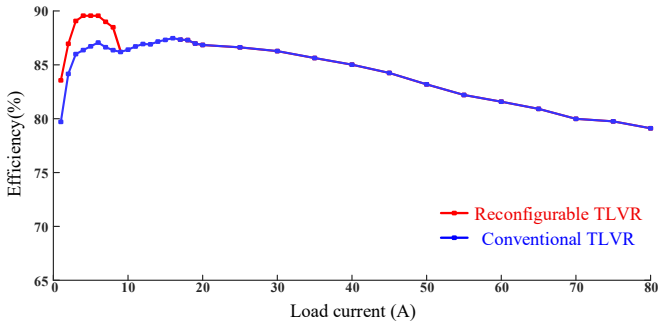

Fig. 8. Efficiency curves for reconfigurable TLVR and conventional TLVR.

V. Experimental Results

To validate the efficiency improvement of the proposed scheme compared to the conventional TLVR, a 12V/1.8V, 500kHz, 80A 4-phase reconfigurable TLVR is designed and tested, as shown in Fig. 7. The critical parameters are listed in Table I. Both the magnetizing inductance L_m and the compensation inductance L_c are 200nH. From (3) - (5), L_{nc} is calculated as 205nH and L_{ss} is 180.7nH. Conventional TLVR operation is simulated by keeping the secondary switch turned on. The light load is defined as less than 10% of the full load, corresponding to output currents below 8A. To better observe the efficiency comparison at light load, additional test points are taken when the load current is below 20A. The efficiency curves for both configurations are plotted in Fig. 8.

As shown in Fig. 8, the reconfigurable TLVR exhibits higher efficiency than the conventional TLVR. As the load current decreases to below 8A, the efficiency of the conventional TLVR behaves as shown by the blue curve, due to phase shedding. In contrast, the reconfigurable TLVR achieves a higher efficiency, as represented by the red curve. This agrees well with the theoretical analysis. The full load efficiency is approximately 80%. The peak efficiency occurs at an output current of 4A, reaching 89.6%. The experimental waveforms for this condition are shown in Fig. 9.

Fig. 9 shows a comparison of the inductor currents for the reconfigurable TLVR and the conventional TLVR. As seen in the figure, when the converter operates at light load and phase shedding is employed, induced current flows in the OFF phases of the conventional TLVR. With the proposed method,

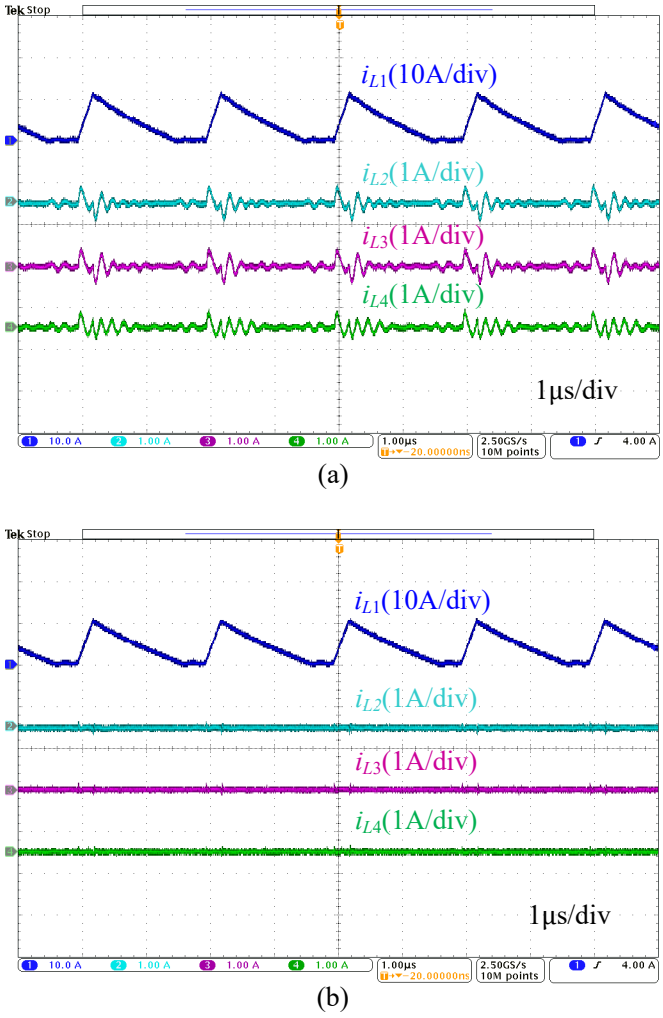

Fig. 9. Experiment waveforms at 4A output current (phase shedding):(a) Conventional TLVR. (b) Reconfigurable TLVR with secondary switch turned off.

this induced current is almost eliminated, resulting in reduced current ripple. Consequently, the light load efficiency improves from 86.4% to 89.6%. For each point between 1A and 8A of output current, the average efficiency improvement is 2.9%.

VI. Conclusion

This paper proposes a reconfigurable method to enhance the light load efficiency of TLVRs. By incorporating an additional secondary switch to control the coupling between phases, the proposed scheme maintains the high transient response of conventional TLVRs under heavy loads while significantly improving efficiency at light loads. Experimental results confirm that phase decoupling enhances the effectiveness of phase shedding, reduces current ripple, and achieves an average light load efficiency improvement of 2.9%. This method offers a promising approach for improving the overall performance of TLVRs in light load conditions.

References

[1] Supermicro, "Top ten best practices for a green data center," https://www.supermicro.com/white_paper/Top_10_Best_Practices_for_a_Green_Data_Center.pdf, 2022, online; accessed October 17, 2024.

[2] J. Liang and H. Wang, "Light load efficiency boost technique for switched tank converters based on hybrid zvs-zcs control," in *Proc. Int. Power Electron. Conf. (IPEC-ECCE Asia)*. IEEE, May 2022, pp. 2231–2235.

[3] S. Jiang, X. Li, M. Yazdani, and C. Chung, "Driving 48v technology innovations forward - hybrid converters and trans-inductor voltage regulator (tlvr)," in *Proc. IEEE Appl. Power Electron. Conf. Expo. (APEC)*, New Orleans, LA, Mar. 2020.

[4] N. Zhang, C. Zhan, G. Ye, C. Chen, X. Li, and J. Yi, "Analysis of multi-phase trans-inductor voltage regulator with fast transient response for large load current applications," in *Proc. IEEE Int. Symp. Circuits Syst. (ISCAS)*, May 2021, pp. 1–5.

[5] J. Sun, M. Xu, Y. Ren, and F. C. Lee, "Light-load efficiency improvement for buck voltage regulators," *IEEE Trans. Power Electron.*, vol. 24, no. 3, pp. 742–751, Mar. 2009.

[6] J. Liang, L. Wang, M. Fu, J. Liang, and H. Wang, "Overview of voltage regulator modules in 48 v bus-based data center power systems," *CPSS Trans. Power Electron. Appl.*, vol. 7, no. 3, pp. 283–299, 2022.

[7] I. A. Mashhadi, B. Soleymani, E. Adib, and H. Farzanehfard, "A dual-switch discontinuous current-source gate driver for a narrow on-time buck converter," *IEEE Trans. Power Electron.*, vol. 33, no. 5, pp. 4215–4223, 2017.

[8] M. Biswas, S. Majhi, and H. B. Nemade, "A high step-down dc–dc converter with reduced inductor current ripple and low voltage stress," *IEEE Trans. Ind. Appl.*, vol. 57, no. 2, pp. 1559–1571, 2020.

[9] Y. Ren, M. Xu, K. Yao, and F. C. Lee, "Two-stage approach for 12-v vr," *IEEE Trans. Power Electron.*, vol. 19, no. 6, pp. 1498–1506, 2004.

[10] M. Veerachary, "Two-switch semiquadratic buck converter," *IEEE Trans. Ind. Electron.*, vol. 64, no. 2, pp. 1185–1194, 2016.

[11] L. Wang, C. Li, J. Liang, and H. Wang, "A multi-phase series capacitor trans-inductor voltage regulator with high switching frequency and fast dynamic response," in *Proc. IEEE Appl. Power Electron. Conf. Expo. (APEC)*, Orlando, FL, Mar. 2023.

[12] C. Li, L. Wang, G. Zheng, M. Fu, and H. Wang, "Small-signal modeling and loop analysis of ultrafast series capacitor trans-inductor voltage regulator with constant on-time control," *IEEE Trans. Power Electron.*, in press, DOI: 10.1109 / TPEL. 2024.3488734.

[13] C. Tu, R. Chen, and K. D. Ngo, "Steady-state analysis of series-resonator buck converter," *IEEE Trans. Power Electron.*, vol. 37, no. 10, pp. 12 327–12 335, 2022.

[14] D. A. Grant, Y. Darroman, and J. Suter, "Synthesis of tapped-inductor switched-mode converters," *IEEE Trans. Power Electron.*, vol. 22, no. 5, pp. 1964–1969, 2007.

[15] T. Yao, M. Ban, and Y. Liu, "A high conversion ratio converter based on tapped-series capacitor circuit," *IEEE Trans. Power Electron.*, 2024.

[16] B. Soleymani, O. Bagheri, E. Adib, and S. Eren, "A zvs high step-down converter with reduced component count and low ripple output current," *IEEE Open J. Power Electron.*, 2024.

[17] Y. Dong, Y. Yang, F. C. Lee, and M. Xu, "The short winding path coupled inductor voltage regulators," in *Proc. IEEE Appl. Power Electron. Conf. Expo. (APEC)*, Austin, TX, USA, Feb. 2008, pp. 1446–1452.

[18] J. Kaiser and T. Duerbaum, "An overview of saturable inductors: Applications to power supplies," *IEEE Trans. Power Electron.*, vol. 36, no. 9, pp. 10 766–10 775, 2021.

[19] F. Li, L. Wang, B. Wu, L. Yu, and K. Wang, "A novel planar nonlinear coupled inductor for improving light and intermediate load efficiency of dc/dc converters," *IEEE J. Emerg. Sel. Topics Power Electron.*, vol. 11, no. 2, pp. 2004–2014, Apr. 2023.

[20] M. A. Alharbi, A. M. Alcaide, M. Dahidah, P. Montero-Robina, S. Ethni, V. Pickert, and J. I. Leon, "Rotating phase shedding for interleaved dc–dc converter-based evs fast dc chargers," *IEEE Trans. Power Electron.*, vol. 38, no. 2, pp. 1901–1909, 2022.

[21] J.-T. Su and C.-W. Liu, "A novel phase-shedding control scheme for improved light load efficiency of multiphase interleaved dc–dc converters," *IEEE Trans. Power Electron.*, vol. 28, no. 10, pp. 4742–4752, Oct. 2013.

[22] F. Zhu and Q. Li, "Coupled inductors with an adaptive coupling coefficient for multiphase voltage regulators," *IEEE Trans. Power Electron.*, vol. 38, no. 1, pp. 739–749, Jan. 2023.